CRYSTAL GROWTH & DESIGN

pubs.acs.org/crystal

Article

Widening the Scope of Structural Correlations by Means of the van der Waals Crust Penetration Indices: The Dimerization of Groups 11 and 12 L−M−X Halo Complexes

Published as part of Crystal Growth & Design virtual special issue "Legacy and Future Impact of the Cambridge Structural Database: A Tribute to Olga Kennard".

Jorge Echeverría and Santiago Alvarez*

Cite This: https://doi.org/10.1021/acs.cgd.4c00335

Read Online

ACCESS | Metrics & More | Article Recommendations | Supporting Information

ABSTRACT: We present in this paper the application of the recently proposed interpenetration indices of the van der Waals crusts to the study of incipient bonds between metal atoms of groups 11 or 12 with halide atoms. To that end, we have carried out a structural database analysis of three-coordinate complexes with a metal halide (M−X) bond and of two-coordinate complexes with a secondary M···X interaction, including the path of formation of LM(μ-X)$_2$ML dimers. The structural data for 18 combinations of metal and halide can be represented by a unique path that correlates the L−M−X (or M···X) bond angle with the M−X (or M···X) penetration index.

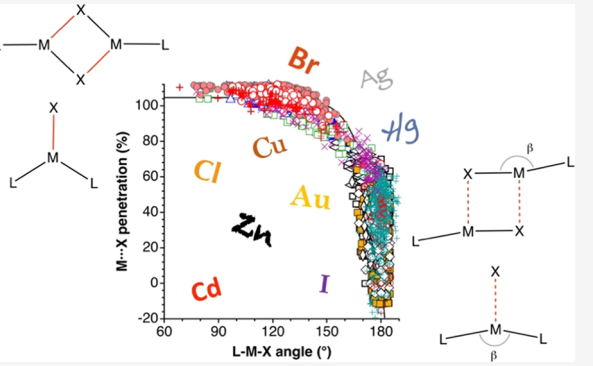

One of the fields that has most benefited from the visionary endeavor of Olga Kennard[1] is that of Structure Correlations, successfully explored by Bürgi and Dunitz,[2−4] Brammer,[5,6] Orpen,[7] and many others,[8] which allows us to interpret the correlation between two structural parameters within a family of related compounds as providing snapshots of chemical reaction pathways.[9] Some paradigmatic examples include the proton transfer reaction showcased by O−H···O hydrogen bonds and the S_N2 nucleophilic substitution mechanism at Sn atoms represented by the structures of X-SnR_3···Y, X-SnR_3-Y, and X···R_3Sn−Y compounds, where the dotted lines indicate nonbonding short contacts or incipient bonds.[10]

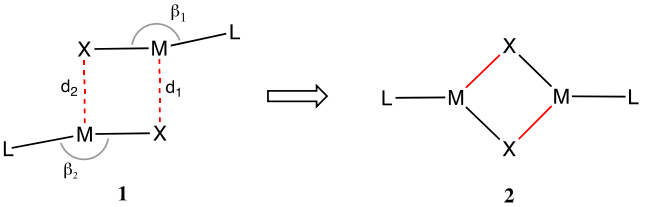

1 2

In an earlier research carried out in our group,[11] we found a structural correlation for Cu(I) linear complexes of general formula L−Cu−X (where X is a halogen), which describes a pathway that takes from weakly associated dimers (**1**), at long intermolecular Cu···X distances, to fully bonded dimers (**2**) with angles β of around 120° and short Cu···X distances. An updated version of such correlations, obtained from the current structural data at the CSD,[12] is shown in Figure 1a, for which we have disregarded the weakly bound dimers whose intermolecular Cu···X distances are longer than the Cu···Cu one (**3**), that are most likely held by metallophilic interactions.[13] There, we see that the nearly linear L−M−X molecules form the longest contacts and that the three different halogen atoms found in those compounds present practically parallel trends.

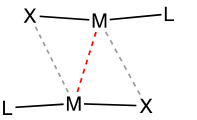

3

We have recently proposed[14,15] to analyze *penetration indices* rather than raw interatomic distances when comparing bonds of varying strengths and involving different pairs of atoms. We defined the van der Waals crust of a given element as the space comprised between a sphere with the van der Waals radius and

Received: March 5, 2024
Revised: April 10, 2024
Accepted: April 10, 2024

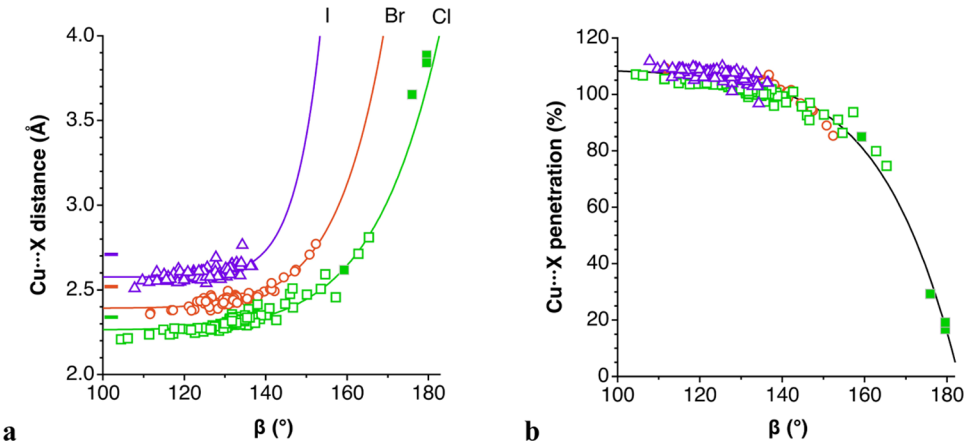

Figure 1. (a) Dependence of the Cu···X distance on the L−Cu−X bond angle (X = Cl, Br, I) describing the path for the dimerization of linear [LCuX] complexes. The solid symbols correspond to compounds retrieved from the CSD as monomers with intermolecular contacts (**1**), and empty symbols to compounds found as bonded dimers (**2**); the marks on the left axis indicate the covalent radii sums.[16] (b) Cu···X penetration indices for the same data set represented as a function of the bond angle. The solid line represents a least-squares fitting to a power function (eq 2).

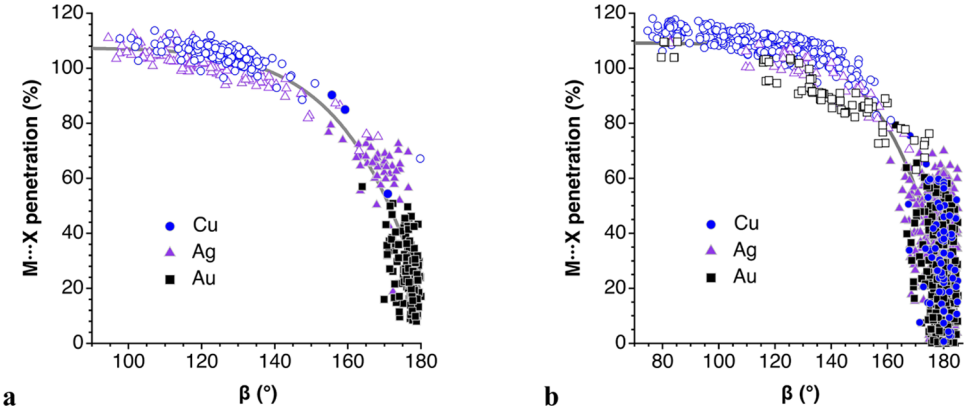

Figure 2. Scatterplot of the M−X penetration index (M = Cu, Ag, Au; X = Cl, Br, I) and the bond angle β in **1** or **4** (L is a nonhalogen two-electron donor): (a) between two L−M−X monomers **1** or **2**, and (b) in three-coordinate compounds **5** or in two-coordinate complexes with a short contact to a halogen **4**. The filled symbols are used for compounds coded in the CSD as intermolecular contacts **1** or **4**, and empty symbols for those coded as bonded species **2** or **5**. The solid lines are least-squares fitting of all of the data in each plot to eq 3 (fitting parameters in Table 1).

Table 1. Parameters for the Least-Squares Fitting of the Data Sets Represented in Figures 1−3 and Eq 3[a]

systems	M	p_0	A	N	
$(L-M-X)_2$	Cu	107.9	4.489	455	Figure 1
L_2M-X	Cu, Ag, Au	107.4	4.511	1330	Figure 2a
	Cu, Ag, Au	109.2	4.462	1620	Figure 2b
$(L-M-X)_2$, L_2M-X	Cu, Ag, Au, Zn, Cd, Hg	102.4	3.514	4374	Figure 3

[a] N is the number of data of each set.

the inner sphere with the covalent radius of an atom. Then, the penetration index p_{AB} for an A−B atom pair calibrates the percentage of interpenetration of the two crusts that can be straightforwardly calculated from the interatomic distance d_{AB}, the covalent radii[16] r_A and r_B, and the van der Waals radii[17] v_A and v_B (eq 1). Such a proposal is tested here for the family of covalent or noncovalent bonds between groups 11 or 12 metals with different halides X.

$$p_{AB} = 100 \times (v_A + v_B - d_{AB})/(v_A + v_B - r_A - r_B) \quad (1)$$

The penetration index p_{AB} takes a value of 0% when the two atoms are at a distance equal to the van der Waals radii sum, reaches 100% when they are at bonding distance (i.e., the sum of their covalent radii), and appears at intermediate values for intermediate distances corresponding to weak or noncovalent interactions. Notice that penetration indices can be negative—when the interatomic distance is longer than the van der Waals radii sum—or higher than 100%—when the distance is shorter than the covalent radii sum. The advantage of using penetration indices is that we can compare on equal footing bonds of varying strengths or between different atom pairs. In the present case, the penetration indices should allow us to obtain a general picture of the dimer formation pathway for all of the L−Cu−X complexes. The conversion of interatomic distances into penetration distances transforms the three structural correlations of Figure 1a into a single correlation (eq 2) that encompasses the three halogens (Figure 1b), with the expected

https://doi.org/10.1021/acs.cgd.4c00335
Cryst. Growth Des. XXXX, XXX, XXX−XXX

inversion of the curve due to the negative linear correlation between distance and penetration (eq 1).

$$p_{MX} = 107.9 - 4.489 \times 10^{-19} \cdot \beta^9 \quad (2)$$

We can now go a step further and check if a similar correlation applies for the other group 11 metals, Ag and Au. The results of CSD searches (see the Methodology section) can be easily transformed into M···X penetration indices that are represented as a function of the intramonomer L−M−X angle in Figure 2a. The alignment of points of the nine M−X combinations around a single curve clearly reveals a common pathway for the dimerization of all group 11 linear L−M−X complexes. Still more staggering, the least-squares fittings (eq 3) for the Cu complexes only (Figure 1b) and for the three group 11 metals together (Figure 2a) are very similar, as can be seen in Table 1. Similar fittings can be obtained for each metal independently, with independent plots and the fitting parameters provided as Supporting Information (Figures S1 and S2 and Table S1). The parameters for such an expression are very similar to each other and represent particularly well the behavior for penetration indices higher than 40−50%.

$$p_{MX} = p_0 - A \times 10^{-19} \cdot \beta^9 \quad (3)$$

In addition, a look at Figure 2a reveals different distributions of the structures along the common path for the three coinage metals. The Cu complexes are most commonly found as dimers, but there are many examples of partially associated monomers, covering all of the range of Cu···X penetration indices from 20 to 110%. The Ag complexes present an intermediate behavior with a wide distribution of the Ag···X penetration indices from 20 to 110, and many complexes with penetrations in the range of 50−80%. Finally, the Au complexes do not form full dimers, and the Au···X penetration indices are, in all cases, less than 60%. The near absence of bent Au compounds is consistent with the finding[18] that the energy needed to bend a dicoordinate X-M-L complex (X = Cl, Br, I; M = Cu, Ag, Au; L = NH_3, PH_3) from its linear conformation to a bond angle of 120° that allows for the coordination of a third ligand is much higher for gold than for the lighter group 11 metals.

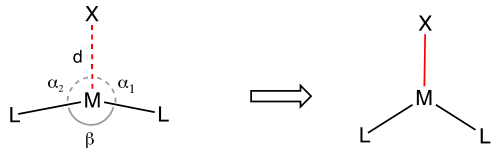

4 5

It is remarkable that the penetration-bond angle correlation holds also for the path of coordination of a third ligand to a dicoordinated metal complex (L_2M−X, **4** to **5** transformation), as can be seen in Figure 2b for the three group 11 metals, and independently in Figures S3 and S4 with the fitting parameters given in Table S1. However, some differences with the dimerization path must be commented upon. (i) There is a wider dispersion of values of the bond angle for the same degree of penetration, which can be attributed to a wider variety of steric and electronic effects in this data set, with almost twice as many structures as that of the $(LM-X)_2$ dimers. (ii) The linearity of the ML_2 group is maintained in this case for penetrations of up to 60%, compared to the dimerization path in which linearity of the monomer is lost at penetrations as low as 45%. Such a difference can probably be attributed to the coincidence of two intermolecular M···X attractive interactions in the dimerization process. (iii) In some cases, we have detected that deviations from the general path can be associated with the presence of more than one short contact to the metal.

An example of the deviations found is provided by a dithiocarbamate gold complex.[19] In its crystal structure, the Au atom and the chloride counterion present an interpenetration of 52% that is associated with a significant bending of the S−Au−S skeleton down to 158°, which is quite larger than expected. However, a closer analysis of the structure reveals that such an interaction is assisted by two NH···Au contacts with H−Au penetrations of 34 and 26%, which explains its anomalous behavior. A similar situation is found for a related compound with a different set of substituents.[20]

Another apparently anomalous behavior is showcased by the salts of the cationic gold complex of a xanthenediphosphine (**6**),[21,22] in which the P−Au−P bond angle is not determined only by the nascent Au···X interaction with a halogen atom (X = Cl, Br, I) of the counteranion but also by the geometrical constraints of the chelating ligand and by a complex pattern of secondary interactions, including Au···O, Au···X, and Au···H (^{t}Bu) contacts with penetrations of around 64, 18, and 34%, respectively, while X···H (^{t}Bu) contacts seem to play a minor role, with penetrations of at most 1%.

Since the group 12 metals also appear commonly in di- or tricoordinated complexes, we have extended our structural study to Zn, Cd, and Hg compounds. The results for compounds **1**, **2**, **4**, and **5**, with M = Zn, Cd, and Hg, and X = F, Cl, Br, and I are shown in Figure 3. Thus, the M−X penetration indices of all of these compounds show the same dependence on the L−M−X bond angle as the analogous compounds of group 11 metals, as seen by comparison with the least-squares fitting curve of Figure 1b (Table 1) that considers the group 11 elements only. The relative scarcity of points in the region with 90% > p > 80% and 150° < β < 160°, clearly suggests that it corresponds approximately to the transition state of the M−X bond-forming reactions. Independent plots and fitting parameters for each metal are provided in Figures S3 and S4 and Table S1. The average fitting parameters for the 12 cases are p_0 = 104(2) giving comparable values for the limiting strong M−X bonds of between 100 and 108% and also similar values for the weighting coefficient of the angular dependence term, A = 3.6(9) It is to be noted, however, that the group 12 structures span a wider range of L−M−X angles. The smallest bond angle (68.5°) and the correspondingly highest penetration (110%) appear for a Zn tricoordinated iodo complex with a guanidinato chelating ligand (**7**).[23] Similarly, the highest Hg-X penetration (108%) is found for the $[(en)HgI]^+$ cation,[24] with a pretty small chelate N−Hg−N angle of 77.7° (**8**). The penetration values higher than 100% simply result from interatomic distances being smaller than the covalent radii sum.[15] It must be noted also that the structures of dimers 1 and 2 of X−M−X molecules (M = Zn, Cd, Hg; X = F, Cl, Br, I), computationally studied by Donald et al.,[25] nicely fit into the general behavior described here.

CONCLUSIONS

The structural correlation found earlier for the dimerization of dicoordinated halide copper(I) complexes can be extended to Ag and Au analogues as well as to the group 12 metals (Zn, Cd, Hg), under the unifying perspective of the interpenetration of the van der Waals crusts of the M and X atoms of the two monomers. Over 4000 crystallographically independent metal centers are shown to follow, to a good approximation, the same

https://doi.org/10.1021/acs.cgd.4c00335
Cryst. Growth Des. XXXX, XXX, XXX−XXX

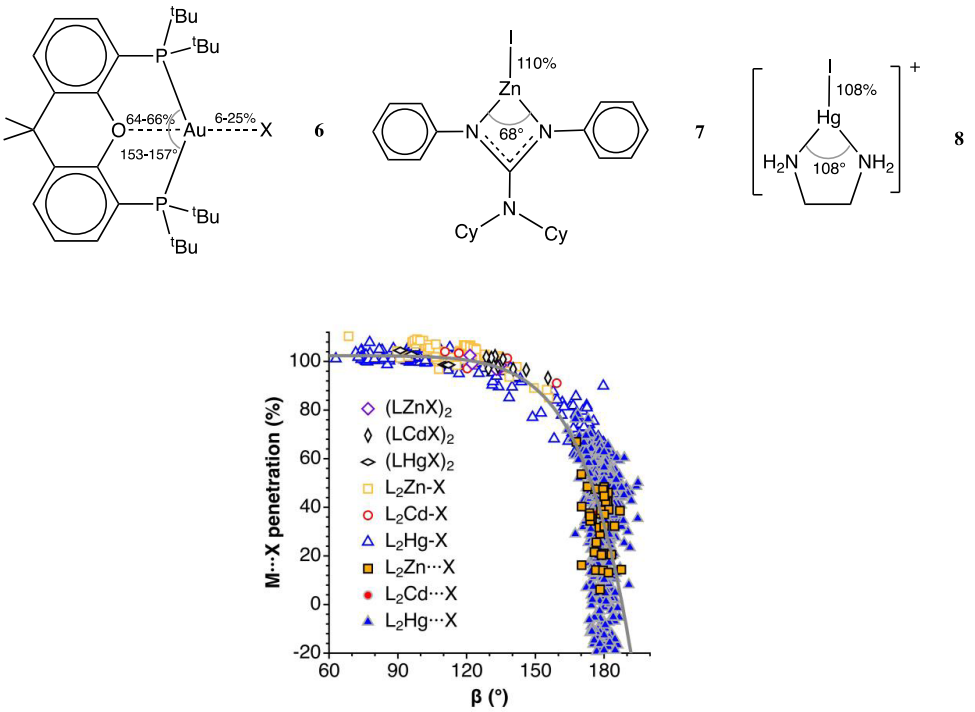

Figure 3. Plot of the M−X and M···X penetration indices between L−M−X monomers as a function of the β bond angle in the $(LMX)_2$ dimers **1** and **2**, and between a dicoordinated complex ML_2 and a bonded or semicoordinated halide X, **4** and **5** (M = Cu, Ag, Au, Zn, Cd, Hg; X = Cl, Br, I; L is a nonhalogen two-electron donor ligand). The solid line represents a least-squares fitting of the full data set to eq 3 (Table 1).

association path from linear dicoordination to trigonal planar coordination for 18 combinations of metal and halide, regardless of the nature of the ancillary ligands.

METHODOLOGY

Structural searches were carried out in the CSD, version 5.45 (November 2023). In all searches, only structures with an *R* factor of at most 7.5% and no disorder were retained for subsequent analysis, except for the cases in which a small data set was obtained with those restrictions. In searches for dimers of type **2**, to get rid of structures with a significant contribution of intermonomer M···M interactions (**3**), the searches were limited to dimers in which the M···M distance exceeds the M···X one by at least 0.1 Å. Since for angles β (**4**) higher than 180°, the L−M−L bond angle given by the CSD is the complementary angle, and therefore β has been calculated as $360°-\alpha_1-\alpha_2$, assuming the ML_2X skeleton to be practically planar. For the searches of structures **4** and **5**, only mononuclear complexes were considered; ligands L were considered to be all groups bonded to the central metal through an element of groups 14−16, with the exception of those of the seventh period. In the case of $L_2M\cdots X$ contacts, the position of the metal atom was restricted to be within ±0.5 Å of the L_2X plane; angle β was limited to values of at most 185°; and systems with negative M···X penetrations were disregarded.

ASSOCIATED CONTENT

Supporting Information

The Supporting Information is available free of charge at https://pubs.acs.org/doi/10.1021/acs.cgd.4c00335.

Individual penetration vs angle plots for each metal atom in $(LMX)_2$ dimers and L_2M-X covalent or incipient bonds, and table with fitting parameters and size of the data sets (PDF)

All of the data used, including CSD refcode, fragment number when there is more than one hit in a particular structure, crystallographic labels for the interacting atoms M and X, bond angle, covalent, and van der Waals radii of the M and X atoms, the calculated penetration index, and a label to indicate whether the M−X atom pair was retrieved as an M−X bond or an M···X contact (XLSX)

AUTHOR INFORMATION

Corresponding Author

Santiago Alvarez − *Department de Química Inorgànica i Orgànica, Secció de Química Inorgànica, e Institut de Química Teòrica i Computacional, Universitat de Barcelona, 08028 Barcelona, Spain;* orcid.org/0000-0002-4618-4189; Email: santiago@qi.ub.es

Author

Jorge Echeverría − *Instituto de Síntesis Química y Catalisis Homogénea (ISQCH) and Departmento de Química Inorgánica, Facultad de Ciencias, Universidad de Zaragoza, 50009 Zaragoza, Spain;* orcid.org/0000-0002-8571-0372

Complete contact information is available at: https://pubs.acs.org/10.1021/acs.cgd.4c00335

Author Contributions

The manuscript was written through contributions of both authors. All authors have given approval to the final version of the manuscript.

Notes

The authors declare no competing financial interest.

https://doi.org/10.1021/acs.cgd.4c00335
Cryst. Growth Des. XXXX, XXX, XXX−XXX

■ ACKNOWLEDGMENTS

This work was supported by the Spanish Ministry of Economy and Competitiveness (PGC2018-093863-B-C21 and PID2022-140244NB-I00) and the Structures of Excellence María de Maeztu program (Grant MDM-2017-0767). J.E. is grateful to the Spanish MICINN for a Ramón y Cajal research contract (RYC-2017-22853).

■ REFERENCES

(1) Hargittai, M. *Women Scientists. Reflexions, Challenges and Breaking Boundaries*; Oxford University Press, 2015.
(2) Bürgi, H. B. Chemical Reaction Coordinates from Crystal Structure Data I. *Inorg. Chem.* **1973**, *12*, 2321−2325.
(3) Bürgi, H. B.; Dunitz, J. D. From Crystal Statics to Chemical Dynamics. *Acc. Chem. Res.* **1983**, *16*, 153−161.
(4) Bürgi, H. B. The Cambridge Structural Database and structural dynamics. *Struct. Dyn.* **2024**, *11*, No. 021302.
(5) Brammer, L. Metals and hydrogen bonds. *Dalton Trans.* **2003**, 3145−3157.
(6) Brammer, L.; Mareque Rivas, J. C.; Spilling, C. D. An intramolecular N−H···Co hydrogen bond and a structure correlation study of the pathway for protonation of the $Co(CO)_3L$ anion (L = CO, PR_3). *J. Organomet. Chem.* **2000**, *609*, 36−43.
(7) Orpen, A. G. Structural Systematics in Molecular Inorganic Chemistry. *Chem. Soc. Rev.* **1993**, *22*, 191−197.
(8) Bürgi, H. B.; Dunitz, J. D. *Structure Correlation*; VCH: Weinheim, 1994.
(9) Mingos, D. M. P. Historical Development of Structural Correlations. *Struct. Bond.* **2020**, *186*, 1−64.
(10) Ruiz-Martínez, A.; Casanova, D.; Alvarez, S. Ligand Association/Dissociation Paths and Ill Defined Coordination Numbers. *Chem. − Eur. J.* **2010**, *16*, 6567.
(11) Liu, X.-Y.; Mota, F.; Alemany, P.; Novoa, J. J.; Alvarez, S. Association of two-coordinate copper(I) complexes: switching on and off Cu···Cu, ligand···ligand and Cu-ligand interactions. *Chem. Commun.* **1998**, 1149−1150.
(12) Groom, C. R.; Bruno, I. J.; Lightfoot, M. P.; Ward, S. C. The Cambridge Structural Database. *Acta Crystallogr., Sect. B* **2016**, *72*, 171−179.
(13) Carvajal, M. A.; Liu, X.-Y.; Alemany, P.; Novoa, J. J.; Alvarez, S. Ligand Effects and Dimer Formation in Dicoordinated Copper(I) Complexes. *Int. J. Quantum Chem.* **2002**, *86*, 100−105.
(14) Gil, D. M.; Echeverría, J.; Alvarez, S. The Tetramethylammonium Cation: Directionality and Covalency in its Interactions with Halide Ions. *Inorg. Chem.* **2022**, *61*, 9082−9095.
(15) Echeverría, J.; Alvarez, S. The borderless world of chemical bonding across the Van der Waals Crust and the valence region. *Chem. Sci.* **2023**, *14*, 11647−11688.
(16) Cordero, B.; Gómez, V.; Platero-Prats, A. E.; Reves, M.; Echeverría, J.; Cremades, E.; Barragán, F.; Alvarez, S. Covalent Radii Revisited. *Dalton Trans.* **2008**, 2832−2838.
(17) Alvarez, S. A Cartography of the Van der Waals Territory. *Dalton Trans.* **2013**, *42*, 8617−8636.
(18) Carvajal, M. A.; Novoa, J. J.; Alvarez, S. Choice of Coordination Number in d^{10} Complexes of Group 11 Metals. *J. Am. Chem. Soc.* **2004**, *126*, 1465−1477.
(19) Schulbert, K.; Mattes, R. Copper and Gold Complexes of Dithiocarbamate Esters. X-Ray Structures of $[CuCl(L^1)_3]\cdot CH_2C1_2$, $[AuCl\ (L^1)]$, $[CuI(L^1)(PPh_3)]_2$ and $[Cu_2^{I}Cu^{II}Cl_4(L^2)_2]_n$ (L^1 = N-Phenyl-S-methyldithiocarbamate, L^2 = N,N-Dimethyl-S-methyldithiocarbamate). *Z. Naturforsch. B* **1993**, *48*, 1227−1233.
(20) Casellato, U.; Fracasso, G.; Graziani, R.; Sindellari, L.; Sánchez-González, A.; Nicolini, M. Gold(I) complexes of thio- and dithiocarbamate esters. The structure of bis(N-methyl-O-ethyl thiocarbamate)gold(I) chloride. *Inorg. Chim. Acta* **1990**, *167*, 21−24.
(21) Ye, X.; Peng, H.; Wei, C.; Yuan, T.; Wojtas, L.; Shi, X. Gold-Catalyzed Oxidative Coupling of Alkynes toward the Synthesis of Cyclic Conjugated Diynes. *Chem* **2018**, *4*, 1983−1993.
(22) Partyka, D. V.; Updegraff, J. B., III; Zeller, M.; Hunter, A. D.; Gray, T. G. Gold(I) halide complexes of bis(diphenylphosphine)-diphenyl ether ligands: a balance of ligand strain and non-covalent interactions. *Dalton Trans.* **2010**, *39*, 5388−5397.
(23) Jones, C.; Furness, L.; Nembenna, S.; Rose, R. P.; Aldridge, S.; Stasch, A. Bulky guanidinato and amidinato zinc complexes and their comparative stabilities. *Dalton Trans.* **2010**, *39*, 8788−8795.
(24) Grdenić, D.; Sikirica, M.; Vickovic, I. Bis(ethylenediamine)-triiododimercury(II) triiodomercurate(II). *Acta Crystallogr., Sect. B* **1977**, *33*, 1630−1632.
(25) Donald, K. J.; Hargittai, M.; Hoffmann, R. Group 12 Dihalides: Structural Predilections from Gases to Solids. *Chem. Eur. J.* **2009**, *15*, 158−177.

https://doi.org/10.1021/acs.cgd.4c00335
Cryst. Growth Des. XXXX, XXX, XXX−XXX